30 degrees Si(g) partial dislocation mobility in nitrogen-doped 4H-SiC

Article *in* Journal of Applied Physics · July 2007

DOI: 10.1063/1.2745266 · Source: IEEE Xplore

4 authors, including:

Hosni Idrissi
Université Catholique de Louvain
63 PUBLICATIONS **848** CITATIONS

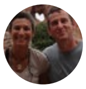

Gabrielle Regula
Aix-Marseille Université
82 PUBLICATIONS **313** CITATIONS

JOURNAL OF APPLIED PHYSICS **101**, 113533 (2007)

30° Si(*g*) partial dislocation mobility in nitrogen-doped 4*H*-SiC

H. Idrissi, B. Pichaud,[a] G. Regula, and M. Lancin
Laboratoire TECSEN UMR 6122 CNRS, Université Paul Cézanne, Aix-Marseille III, Avenue Escadrille Normandie Niemen, 13397 Marseille Cedex 20, France

(Received 21 December 2006; accepted 21 April 2007; published online 13 June 2007)

Well-controlled population of dislocations are introduced in 4*H*-SiC by bending in cantilever mode and annealing between 400 and 700 °C. The introduced defects consist of double stacking faults, each bound by a pair of 30° Si(g) partial dislocations, and the expansion of which is asymmetric. The velocity of each individual 30° Si(g) pair is directly measured as a function of stress and temperature on the surface of samples etched after deformation. The activation energies of the 30° Si(g) partial dislocation pairs are strongly stress dependent, ranging between 1.25 and 1.7 eV. These values are lower than the ones derived from plasticity experiments. This is probably because 30° Si(g) pairs and double stacking faults are generated in N-doped 4*H*-SiC ($N=2\times10^{18}$ cm^{-3}), with their development being promoted by quantum well action. [DOI: 10.1063/1.2745266]

I. INTRODUCTION

4*H*-SiC is a very promising semiconducting material for high power electronics, radiofrequency applications, and more generally for devices that are operated at high temperatures and under high irradiation conditions.[1,2] However, during forward biasing of p-i-n diodes, defects that have been identified as planar defects bound by partial dislocations (PDs), can move over long distances causing electrical degradation after hours or days of constant operation.[3,4] The activation energy of the PD propagation (Q) under such biasing conditions was measured by Galekas *et al.*[5] at low current densities and was found extremely low (≈ 0.27 eV) as compared to what can be estimated from plasticity measurements ($1.8\text{ eV}<E_a<2.5\text{ eV}$) (Refs. 6–8) in the low temperature region. This marked discrepancy was attributed to the recombination-enhanced dislocation glide[9] (REDG) mechanism, that is to a reduction in Q obtained by subtracting the energy of an electron-hole recombination which favors the formation and/or the migration of kinks along the dislocation. Hence it is interesting to directly measure the intrinsic parameters of the dislocation glide (activation energy and stress exponent) under well-controlled biasing or nonbiasing conditions.

Dislocation velocities in semiconductors can be determined either by observation of their movements by *in situ* transmission electron microscopy (TEM) or at a larger scale by measuring the displacement of individual dislocations using double etching or x-ray topography after deformation tests (for review, see Ref. 10). The latter method seems more suitable to achieve conditions similar to those of defect motion in biased diodes. Moreover, with this method the stress state is better controlled, but high perfection crystals are needed to avoid interactions between the dislocations, which would impede their motion over large distances. Finally, the dislocation movements should occur in glide planes as much as possible normal to the surface to avoid image-force effects at their very emerging part. The availability of 4*H*-SiC wafers parallel to the $(11\bar{2}0)$ plane, that is with the (0001) glide plane normal to the surface and with low micropipe and dislocation densities, allows direct measurement of dislocation velocities. Indeed this requires the exclusive use of nitrogen-doped (N-doped) material, since this type of 4*H*-SiC is the only one available with sufficient crystal quality, and suited orientation and thickness.

Moreover, this will also help to understand the recent observation of the development of double stacking faults (DSFs) in highly N-doped 4*H*-SiC submitted to various high temperature device processings.[11–14]

As shown in a previous paper,[15] we were able to nucleate and develop individual 30° Si(g) pairs under a well defined state of stress. These pairs were precisely characterized[15] by chemical etching and TEM in weak beam (WB) and high resolution (HR) imaging modes. Their identification was confirmed by large angle convergent beam diffraction (LACBED).[16]

In the present paper, we report velocity values based on the direct measurement of the PD pair path length as a function of stress and temperature between 400 and 700 °C. The stress exponent m and the activation energy Q can be extracted from the classical law of dislocation velocity v as a function of the stress σ and temperature T,

$$v=A\sigma^m\exp(-Q/kT). \tag{1}$$

The $\{m,Q\}$ values are compared to those deduced from plasticity measurements.[6–8]

II. EXPERIMENT

Rectangular samples ($L=20$ mm; $w=5$ mm; $t=0.25$ mm) were cut from N-doped (2×10^{18} cm^{-3}) 4*H*-SiC wafers purchased from CREE-Research [Fig. 1(a)]. The surface of these samples was parallel to the $(11\bar{2}0)$ plane and their length close to the $[2\bar{2}01]$ direction. In that orientation, the (0001) glide planes were normal to the surface and at 45° from the sample length. Some as-grown specimens were

[a] Electronic mail: bernard.pichaud@univ-cezanne.fr

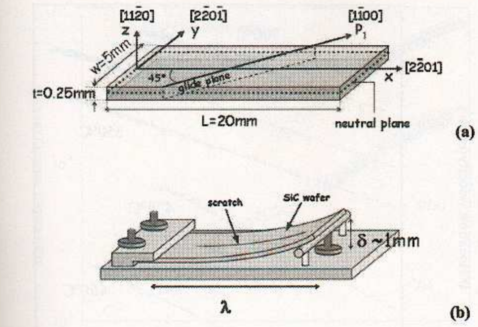

FIG. 1. (a) Geometry of the 4*H*-SiC rectangular sample and (b) bent sample on the deformation holder.

characterized by x-ray transmission topography to verify the absence of micropipe and to obtain information on the initial dislocation density. Figure 2 shows some screw dislocations (S) parallel to the [0001] growth direction and a homogeneous density (mean density of less than 10^4 cm^{-2}) of dislocations in the (0001) glide planes.

Dislocation sources were created by scratching the sample surface in a direction parallel to the sample length using a diamond tip loaded with a 100 *g* weight. The scratch was located at the half-width of the $(11\bar{2}0)$ face [Fig. 1(b)], except when the samples were annealed at 700 °C. In that case, the scratch was performed close to one edge of the sample in order to increase the dislocation paths. The reference axes were chosen so that the $\{X,Y\}$ plane is located at half of the sample thickness (which becomes a neutral plane under stress).

The samples were then bent in cantilever mode at room temperature around the *Y* direction [Fig. 1(b)], resulting in compressive stress on the $(11\bar{2}0)$ face and in tensile stress on the $(\bar{1}\bar{1}20)$ face [see Eqs. (2) and (3) below]. The bent samples were annealed under stress in Ar flux at temperatures ranging from 400 to 700 °C in a conventional furnace. Then the defects were revealed by chemical etching (Fig. 3) with molten KOH (550 °C, 20 min).

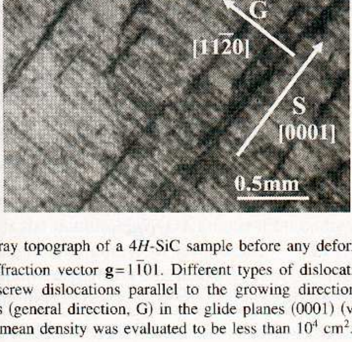

FIG. 2. X-ray topograph of a 4*H*-SiC sample before any deformation procedure. Diffraction vector $\mathbf{g}=1\bar{1}01$. Different types of dislocations can be observed: screw dislocations parallel to the growing direction (S), glide dislocations (general direction, G) in the glide planes (0001) (viewed edge on) whose mean density was evaluated to be less than 10^4 cm^2.

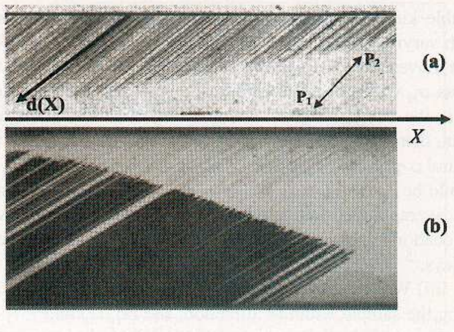

FIG. 3. Optical micrographs after KOH etching showing the regularity of the etching traces parallel to the (0001) glide planes. (a) $(11\bar{2}0)$ face, compressive stress, 550 °C, (b) $(\bar{1}\bar{1}20)$ face, tensile stress, 620 °C. The dislocation path length $d(X)$ is also displayed in (a).

In previous papers,[15,16] it was shown that three different populations of double stacking faults (DSFs) are nucleated from the scratch on the face under compressive stress and develop in the *P*1 direction (DSFAs and DSFBs) or in the opposite *P*2 direction (DSFCs). It was also observed that DFSAs and DSFBs expand on this face from one edge of the sample. Each DSF is dragged by a pair of 30° Si(g) partial dislocation with the same Burgers vector, gliding in adjacent (0001) slip planes and is separated by about 65 nm, whatever the temperature (400–700 °C) or the stress (<200 MPa). Among the three populations, only the DSFAs are driven far from the scratch by the bending stress, giving rise to an asymmetric etched pattern. Indeed, the two 30° Si(g) partial dislocations driving the DSFAs are characterized by a line $\mathbf{L}=[1\bar{2}10]$ and a Burgers vector $\mathbf{b}=a/3[1\bar{1}00]$ and thus are submitted to the highest resolved shear stress $m=0.5$. The measurement of the velocities as a function of the resolved shear stress was performed on these PD pairs.

In the determination of the average shear stress (σ_{ar}) which causes the dislocation motion three aspects must be taken into account.

(i) The variation of the resolved shear stress (σ_r) in a bent sample as a function of *X* and *Z*, that is, $\sigma_r(X,Z)$, has to be measured. This can be done either by recording the local radius of curvature $R(X)$ via the measurement of a laser beam deflection by the sample surface [Eq. (2)] or by measuring the bending amplitude δ [Eq. (3)].

$$\sigma_r(X,Z) = \frac{E}{R(X)} sZ, \qquad (2)$$

$$\sigma_r(X,Z) = \frac{3E}{L^3}\delta sZ(L-X), \qquad (3)$$

where *E* is the Young modulus, *s* the Schmid factor, and *L* the sample length (18 mm in our case).

(ii) We have to take into account that σ_r decreases linearly along the depth and that its sign changes beyond the neutral plane [Eq. (2) and (3)]. Thus, σ_r decreases along the partial dislocation segments as they penetrate deeper into the sample. On the basis of the Hirth and Lothe theory for the double kink movement,[17] it was demonstrated[18] that under such varying stress, in the kink collision regime, the dislocation moves always parallel to the Peierls valleys and that the stress σ_{ar} which must be specifically coupled with the velocity is the average stress undergone by the dislocation segment, that is, the one at halfway between the surface and the neutral plane, $\sigma_{ar}=\sigma_r(X,Z=t/4)=1/2\sigma_r(X,Z=t/2)$. It should be noticed that in the 400–700 °C temperature range this averaging is particularly adequate, since the observed dislocation lines are straight and lying in the Peierls valleys.[15]

(iii) We must consider that although $\sigma_r(X,Z)$ is constant along the sample width [Y direction, see Eq. (2) and (3)] σ_r, and thus σ_{ar}, is not constant in a (0001) glide plane since this plane is inclined at 45° to the X direction. Consequently, the dislocation glide along path d (Fig. 3) takes place under varying stress conditions: in compression as the dislocations move toward lower X values the stress increases linearly, while in tension they move toward lower stress values. The average resolved shear stress on a given dislocation is taken equal to $\sigma_{ar}(X,Z)$ where $X=X_0+d/2\sqrt{2}$, X_0 being the abscissa of the point where the DSFAs are nucleated and $d/2\sqrt{2}$ the projection of point at midlength $d/2$ of the DSFAs on the X axis. The relative uncertainty $\Delta\sigma_{ar}/\sigma_{ar}$ introduced by this estimation is maximum when d is maximum: it can reach ±10% for the experiments at 700 and 620 °C (d_{max} =4.5 mm, scratch performed close to the sample edge) and ±5% for the other temperatures (d_{max}=2.5 mm, scratch performed in the middle of the sample) but drops to ±0.3% for the smallest DSFAs lengths ($d_{min}\sim 130$ μm).

The velocity of a dislocation pair, v, was determined by measuring its wake length d revealed by etching and dividing d by the annealing duration t. The experimental uncertainty on v comes mainly from the evaluation of t. Indeed, despite a special master/slave temperature regulation system, the temperature profile is not a perfect gate function. We estimate this error to vary linearly with the temperature from $\Delta v/v=\pm 5\%$ at 400 °C to $\Delta v/v=\pm 10\%$ at 700 °C.

III. RESULTS

In the present work, it is noteworthy that the envelope of the fault tips is very regular. This is true for the dislocations nucleated from the scratch or from the sample edge, whether the face has been submitted to a compressive stress [Fig. 3(a)] or to a tensile stress [Fig. 3(b)]. This means that the length of the defect is actually determined by a stress dependent velocity and not by the influence of any obstacle, which validates our experimental approach.

The dislocation velocities measured on the $(11\bar{2}0)$ face submitted to a compressive stress are displayed on Fig. 4 as a function of σ_{ar}, for various temperatures. Two distinct stress exponents can be extracted from this figure: m =1.38±0.05 for the highest temperature range (550, 620, and 700 °C) and m=2.1±0.1 for the lowest one (400 and 470 °C). As already suggested,[10] these variations of the stress exponent may be ascribed to stress sensitivity of the dislocation motion activation energy. The Arrhenius plots of the dislocation velocities (sometimes extrapolated from Fig. 4) for different stress levels are presented on Fig. 5, showing a strong variation of the activation energy Q as a function of σ_{ar}.

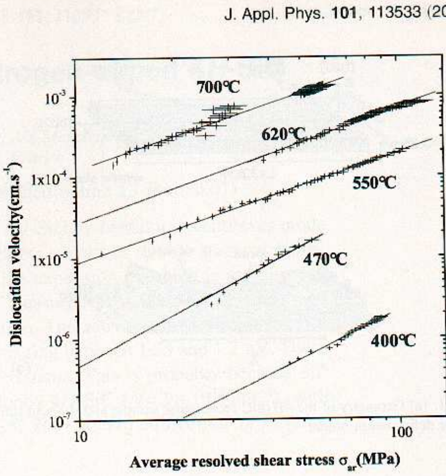

FIG. 4. Velocity measurements of 30° Si(g) partial dislocation pairs as a function of the average resolved shear stress at different temperatures.

Finally, the dislocation velocities measured at 550 and 620 °C on the $(\bar{1}\bar{1}20)$ face submitted to tensile stress are compared to those measured on the $(11\bar{2}0)$ face. The 30° Si(g) PDs dragging the DSFs in the $P2$ direction on the $(\bar{1}\bar{1}20)$ face are characterized by $\mathbf{L}=[1\bar{2}10]$ and $\mathbf{b}$ $=a/3[1\bar{1}00]$. They are submitted to the same forces but their sign as the ones undergone by the DSFAs. The variations of their velocities are within the experimental uncertainty as compared to those measured in compression (Fig. 6).

IV. DISCUSSION

In the 400–700 °C temperature range, only partial dislocations with a silicon core are mobile. We only observed the displacement of 30° Si(g) pairs over large distances because, as already mentioned in literature,[6,19] the 90° Si(g)

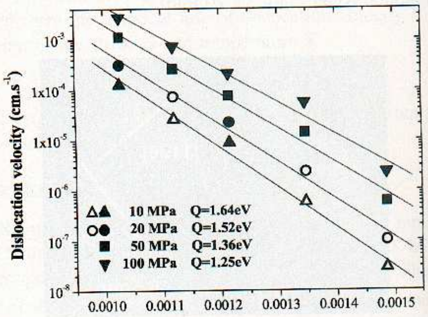

FIG. 5. Arrhenius plots of 30° Si(g) partial pair velocity vs temperature for different average stresses. The activation energy is strongly stress dependent. Full symbols correspond to velocities in the measured ranges and empty symbols are to velocities extrapolated using the dotted lines in Fig. 4.

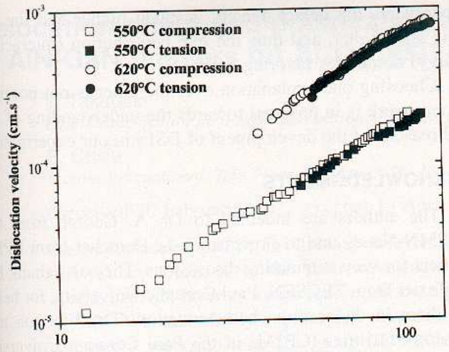

FIG. 6. Comparison of dislocation velocities in tension (full symbols) or compression (empty symbols) modes at 550 and 620 °C.

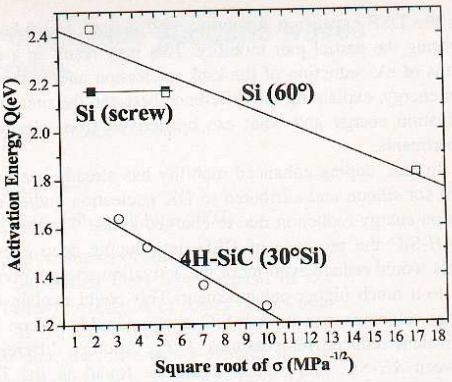

FIG. 7. Evolution of the activation energy for the 30° Si(g) partial pair velocity as a function of the square root of the effective stress. Literature results for dislocations in silicon (Ref. 22 and 25) are also displayed.

partial dislocations are so fast that they leave the sample even before annealing is completed. Hence, we measured the velocities of these 30° Si(g) partial pairs. This does not mean that C core dislocations are never observed. Indeed, C core segments are produced when the PDs move over long distances, but they will never drive a dislocation loop. So our observations yield the following hierarchy for dislocation velocities: $V_{\mathrm{Si}}^{90°} > V_{\mathrm{Si}}^{30°} > V_{\mathrm{C}}^{90°-30°}$, in agreement with former experimental works but in contradiction with what is predicted from the activation energies obtained by *ab initio* calculations.[20,21]

The partial dislocation velocities measured in this work are very high, especially if compared with those obtained in silicon (if such comparison were possible). A 30° Si(g) partial pair in 4*H*-SiC and the perfect screw dislocation in Si (Ref. 22) [made up of two 30° Si(g)] have similar velocities, between 10^{-7} and 10^{-4} cm s^{-1}, at 30 MPa in quite different temperature domains (in unit of melting temperature T_m), typically $0.2T_m<T<0.3T_m$ for SiC and $0.4T_m<T<0.6T_m$ for Si. Eventually the difference in cohesive energy between SiC and Si [6.34 eV/atom (Ref. 23) and 4.63 eV/atom (Ref. 24), respectively] should allow us to speculate for the lowest dislocation mobility in 4*H*-SiC. The question is: What helps the dislocation glide at such low temperatures in 4*H*-SiC? Possible answers will be proposed later on.

The glide activation energy of a 30° Si(g) pair is very sensitive to the stress (see Fig. 5). A decrease in the activation energy with the increasing resolved shear stress was predicted by Hirth and Lothe.[17] In the case of the kink collision regime, the activation energy Q may be decomposed as

$$Q = F^*/2 + W_m, \tag{4}$$

where F^* is the double kink (DK) nucleation energy and W_m the kink migration energy. At low stress, $F^* \approx 2F_k$, F_k being the nucleation energy of a single kink. At high stress, F^* and thus Q are reduced by a term accounting for the stress influence,[17]

$$F^* = 2F_k - \left(\frac{\mu\sigma_r b^3 h^3}{2\pi}\right)^{1/2} \tag{5}$$

and

$$Q = F_k + W_m - \left(\frac{\mu\sigma_r b^3 h^3}{8\pi}\right)^{1/2} = Q_0 - A\sqrt{\sigma_r}, \tag{6}$$

with μ the shear modulus, σ_r the resolved shear stress, b the Burgers vector modulus, and h the distance between two successive Peierls valleys.

On Fig. 7, the activation energy variations are drawn as a function of the square root of the revolved shear stress. The law expressed in Eq. (6) is reasonably well verified by the activation energies obtained in the present work. The Q variations shown on Fig. 7 for silicon[22,25] exhibit a similar behavior (60° dislocations). Other results on the stress dependence of Q are available in the literature for elemental semiconductors[22,26,27] but we will not mention them here since they concern a too narrow stress range. On Fig. 7, it could be noticed that the low stress activation energy $Q_0 = F_k + W_m$ is close to 1.7 eV in 4*H*-SiC. Of course, as in these experiments we were always in the case of the kink collision regime, so it is impossible to evaluate separately the two contributions (nucleation and migration). Nevertheless, the activation energy for low stress is found somewhat below the range expected from plasticity experiments, 1.8–2.5 eV.[6–8] The well-known recombination-enhanced mobility mechanism cannot be invoked here to explain this reduction in activation energy since it would need ultraviolet light that obviously we did not use. In fact, we measured the mobility of individual partial dislocation pairs while in plasticity experiments, and within the same temperature range, numerous single partial dislocations are involved. One 30° Si(g) pair drives a DSF, whose associated energy level is located in the band gap 0.6–0.7 eV below the conduction band.[11,28,29] In N-doped 4*H*-SiC, like the one we used in this work ($N=2\times10^{18}$ cm^{-3}), the Fermi level drops between $E_c-0.18$ eV and $E_c-0.31$ eV as T increases (400–700 °C), leading to highly probable electron transfer toward the DSF level, easing the DSF expansion (quantum well action[12]) and hence favoring the partial pair mobility. This may result in a few tenths of eV reduction of the kink nucleation and/or migration energy, explaining the difference between the measured activation energy and what can be derived from plasticity experiments.

In fact, doping enhanced mobility has already been noticed for silicon and attributed to DK nucleation and/or migration energy reduction due to charged kinks.[30] In the case of 4*H*-SiC the presence of DSFs introducing deep energy levels would reduce even more the activation energy, giving rise to a much higher enhancement. This could explain the higher velocities measured in SiC as compared to silicon for equivalent reduced temperatures T/T_m. Another difference between 4*H*-SiC and silicon could be found in the DK mechanisms occurring on a dissociated perfect dislocation (Si) and on a pure partial dislocation (SiC). As a matter of fact, in silicon, due to the presence of two partial dislocations separated by a relatively high energy fault, kink pairs must form in both partials in a correlated manner[31] [at least for stresses below 20 MPa (Ref. 10)] in order to promote a neat motion of the line, while in a pure partial dislocation this requirement does not actually exist. This can result in an intrinsically lower mobility for the pure partial dislocation than for a dissociated perfect one. Obviously, both mechanisms, quantum well action or difference in DK formation, can cooperate to induce surprising low dislocation velocities in 4*H*-SiC.

Of course, since many points in this discussion are related to the quantum well action which is supposed to play a role in N-doped 4*H*-SiC, it would be of fundamental interest to measure dislocation velocities in undoped or low doped 4*H*-SiC, but unfortunately it is quite impossible since this type of material is only available as thin films.

We also have to understand why, for very similar 4*H*-SiC (same doping impurity N and similar doping level), only partial dislocation pairs are involved in our work, whereas only single partial dislocations are involved in plasticity experiments. Two possible reasons may be given for this: (i) In our case the particular procedure for dislocation nucleation from a scratch at the surface; it may favor (for unknown reasons) the partial dislocation pairs and the DSF that follows, whereas in plasticity experiments the nucleation of dislocations takes place in the bulk, involving single faulted loops (SSF). (ii) The relative amount of the stacking fault energy and the elastic energy due to the dislocation interaction; if we compare DSF and SSF for an equivalent shear amount, that is, one DSF and two SSFs having the same surface, the advantage for the DSF is a gain in stacking fault energy, $\gamma_1+\gamma_2$ instead of $2\gamma_1$ for both SSFs, where $\gamma_1 = (1.5-1.8)\times 10^{-2}$ J m^{-2} (Refs. 32 and 33) and γ_2 being the energy of the second SF when the first already exists, $\gamma_2 = 0.3\times 10^{-2}$ J m^{-2}.[33] The disadvantage is the increase in elastic energy corresponding to the interaction of the very close partials bounding the DSF. The relative weight of these contributions depends on the size of the defect (SSF or DSF). For very low defect density and very large defects as in our case, the surface contribution (stacking fault energy) dominates and the DSFs are more stable, whereas in plasticity experiments the defect density is much higher and the defects are smaller, and thus the line contribution (interaction energy) dominates favoring SSFs.

Choosing one explanation over the other is not possible yet but work is in progress towards the understanding of the real reasons of the development of DSFs in our experiments.

ACKNOWLEDGMENTS

The authors are indebted to Dr. A. George from the ENSMN-Nancy and to Professor J.-L. Demenet from LPM-Poitiers for very stimulating discussions. They also thank Dr. M. Texier from TECSEN, Paul Cezanne University, for helping them in dislocation characterization. The Electron microscopy facilities (CP2M) of the Paul Cézanne University are also greatly acknowledged.

[1] P. G. Neudeck, R. S. Okojie, and L.-Y. Chen, Proc. IEEE **90**, 1065 (2002).
[2] R. Rupp and I. Zverev, Mater. Sci. Forum **433–436**, 805 (2003).
[3] H. Lendenmann, F. Dahlquist, N. Johansson, R. Soderholm, P. A. Nilsson, J. P. Bergman, and P. Skytt, Mater. Sci. Forum **353–356**, 727 (2001).
[4] J. P. Bergman, H. Lendenmann, P. A. Nilsson, U. Lindefelt, and P. Skytt, Mater. Sci. Forum **353–356**, 299 (2001).
[5] A. Galeckas, J. Linnros, and P. Pirouz, Appl. Phys. Lett. **81**, 883 (2002).
[6] A. V. Samant, M. H. Hong, and P. Pirouz, Phys. Status Solidi B **222**, 75 (2000).
[7] J. L. Demenet, M. H. Hong, and P. Pirouz, Mater. Sci. Forum **338–342**, 517 (2000).
[8] J. L. Demenet, M. H. Hong, and P. Pirouz, Scr. Mater. **43**, 865 (2000).
[9] K. Maeda and S. Takeuchi, *Dislocations in Solids*, edited by H. Suzuki, T. Ninomiya, K. Sumino, and S. Takeuchi (University of Tokyo Press Tokyo, 1985), p. 433.
[10] A. George and J. Rabier, Rev. Phys. Appl. **22**, 941 (1987).
[11] R. S. Okojie, M. Xang, P. Pirouz, S. Tumakha, G. Jessen, and L. J. Brillson, Appl. Phys. Lett. **79**, 3056 (2001).
[12] J. Q. Liu, H. J. Chung, T. Kuhr, Q. Li, and M. Skowronski, Appl. Phys. Lett. **80**, 2111 (2002).
[13] H. J. Chung, J. Q. Liu, and M. Skowronski, Appl. Phys. Lett. **81**, 3759 (2002).
[14] M. Zhang, H. M. Hobgood, M. Treu, and P. Pirouz, Mater. Sci. Forum **457–460**, 759 (2004).
[15] G. Regula, M. Lancin, H. Idrissi, B. Pichaud, and J. Douin, Philos. Mag. Lett. **85**, 259 (2005).
[16] M. Texier, G. Regula, M. Lancin, and B. Pichaud, Philos. Mag. Lett. **86**, 235 (2006).
[17] J. P. Hirth and J. Lothe, *Theory of Dislocations* (Kreiger, Malabar, FL, 1992), p. 531.
[18] B. Pichaud, P. Jean, and F. Minari, Philos. Mag. A **54**, 479 (1986).
[19] P. Pirouz and J. W. Yang, Ultramicroscopy **51**, 189 (1993).
[20] P. K. Stich, R. Jones, S. Oberg, and M. I. Heggie, Phys. Rev. B **52**, 4951 (1995).
[21] A. T. Blumenau, R. Jones, S. Oberg, P. R. Briddon, and T. Frauenheim, Physica B **340–342**, 160 (2003).
[22] A. George and G. Champier, Phys. Status Solidi A **53**, 529 (1979).
[23] K. J. Chang and M. L. Cohen, Phys. Rev. B **35**, 8196 (1987).
[24] *Physics of Group IV Elements and III-V Compounds*, edited by O. Madelung, Landolt-Börnstein, New Series, Group III, Vol. 17, Pt. A (Springer, Berlin, 1982).
[25] K. H. Küsters and H. Alexander, Physica B **116**, 594 (1983).
[26] M. Imai and K. Sumino, Philos. Mag. A **47**, 599 (1983).
[27] H. Schaumburg, Philos. Mag. **25**, 1429 (1972).
[28] B. J. Skromme, K. Palle, C. D. Poweleit, L. R. Bryant, W. Vetter, M. Dudely, K. Moore, and T. Gehoski, Mater. Sci. Forum **389–393**, 455 (2002).
[29] H. P. Iwata, U. Lindefelt, S. Oberg, and P. R. Briddon, Mater. Sci. Forum **389–393**, 493 (2002).
[30] P. Haasen, J. Phys. Colloq. **44**, C3–149 (1981).
[31] H. J. Möller, Acta Metall. **26**, 963 (1978).
[32] M. H. Hong, A. Samant, and P. Pirouz, Philos. Mag. A **80**, 919 (2000).
[33] H. P. Iwata, U. Lindefelt, S. Oberg, and P. R. Briddon, J. Appl. Phys. **93**, 1577 (2003).